JOURNAL OF AIRCRAFT
Vol. 43, No. 5, September–October 2006

Conceptual Design and Simulation of a Small Hybrid-Electric Unmanned Aerial Vehicle

Frederick G. Harmon,* Andrew A. Frank,† and Jean-Jacques Chattot‡
University of California—Davis, Davis, California 95616-5294

DOI: 10.2514/1.15816

Parallel hybrid-electric propulsion systems would be beneficial for small unmanned aerial vehicles used for military, homeland security, and disaster-monitoring missions involving intelligence, surveillance, or reconnaissance (ISR). The benefits include increased time on station and range as compared to electric-powered unmanned aerial vehicles and reduced acoustic and thermal signatures not available with gasoline-powered unmanned aerial vehicles. A conceptual design of a small unmanned aerial vehicle with a parallel hybrid-electric propulsion system, the application of a rule-based controller to the hybrid-electric system, and simulation results are provided. The two-point conceptual design includes an internal combustion engine sized for cruise speed and an electric motor and lithium-ion battery pack sized for endurance speed. A rule-based controller based on ideal operating line concepts is applied to the control of the parallel hybrid-electric propulsion system. The energy use for the 13.6 kg (30 lb) hybrid-electric unmanned aerial vehicle with the rule-based controller during one-hour and three-hour ISR missions is 54% and 22% less, respectively, than for a four-stroke gasoline-powered unmanned aerial vehicle.

Nomenclature

AR	=	aspect ratio
C_D	=	total drag coefficient
$C_{D,0}$	=	zero-lift drag coefficient
C_L	=	lift coefficient
$C_{L,\max}$	=	maximum lift coefficient
e	=	Oswald efficiency factor
$e(t)$	=	speed error signal, m/s
J	=	objective function to be minimized
m	=	mass, kg or lbs
P_{EM}	=	power output of the electric motor, W
P_{ICE}	=	power output of the internal combustion engine, W
PR	=	power required, W
S	=	wing area, m^2
TR	=	thrust required, N
$u(t)$	=	controller command signals
V_{Cruise}	=	cruise speed, m/s or kn
$V_{\mathrm{Endurance}}$	=	endurance speed, m/s or kn
V_{Stall}	=	stall speed, m/s or kn
W	=	weight of UAV, N or lbs
W_{Empty}	=	empty weight, N or lbs
W_{Fuel}	=	fuel weight, N or lbs
W_0	=	gross takeoff weight, N or lbs
W_{Payload}	=	payload weight, N or lbs
$W_{\mathrm{Propulsion}}$	=	propulsion system weight, N or lbs
$y(t)$	=	output signal, UAV speed, m/s
η_{Prop}	=	propeller efficiency
ρ	=	air density, kg/m^3

Received 27 January 2005; revision received 2 February 2006; accepted for publication 14 February 2006.

*Graduate Student, Department of Mechanical and Aeronautical Engineering, One Shields Avenue.
†Professor, Department of Mechanical and Aeronautical Engineering.
‡Professor and Vice Chairman, Department of Mechanical and Aeronautical Engineering, Member AIAA.

I. Introduction

A hybrid-electric vehicle (HEV) is "a vehicle in which propulsion energy is available from two or more kinds or types of energy stores, sources, or converters, and at least one of them can deliver electrical energy [1]." Within the automotive industry, HEV technology is leading to vehicles with increased fuel economy and reduced emissions. The same technology would have similar benefits if applied to unmanned aerial vehicles (UAVs) used for military, homeland security, and disaster-monitoring missions involving intelligence, surveillance, and reconnaissance (ISR). Because of the hybrid and electric-only modes, the potential benefits include increased time on station, longer range, and reduced signature. A parallel hybrid-electric propulsion system for a small UAV provides increased time on station and longer range as compared to electric-powered UAVs such as the Dragon Eye or Desert Hawk [2]. The internal combustion engine (ICE) is downsized for steady-state conditions and operated near a constant torque output. The electric motor (EM) provides additional power for acceleration or climbing and serves as a generator during charge-sustaining operation or regeneration. Electric-only operation reduces the acoustic, smoke, and thermal signatures as compared to gasoline-powered UAVs [3]. Also, electric-only operation eliminates exhaust emissions that could interfere with chemical-detecting sensors. The battery pack/generator that usually provides power for the avionics, flight control system, and payload also provides propulsion power during certain flight phases. The electric system also provides redundancy for the gasoline engine and reduces the risk of losing expensive payloads while the UAV is operating in hazardous conditions. Because of these advantages, a small UAV with a parallel hybrid-electric propulsion system would enhance specific types of missions.

The Defense Advanced Research Projects Agency (DARPA) and other agencies are considering hybrid-electric propulsion systems for UAVs. DARPA's Micro Air Vehicle (MAV) project is designed to give the Army or Special Operations Forces a UAV with a reconnaissance and surveillance capability [4]. The MAV is a vertical takeoff and landing vehicle utilizing ducted fan technology. A series hybrid-electric propulsion system that includes a diesel engine, generator, electric motor, and battery pack has been considered for the MAV. DARPA has also given a contract to Boeing to consider a fuel cell-based hybrid-electric propulsion system for a UAV [5]. This Ultra Leap project was proposed to have military as well as civilian applications. An example of a civilian application is Helios, NASA's high-altitude, long-endurance UAV developed by AeroVironment, which is designed for telecommunications and

atmospheric monitoring [6]. The Israel Institute of Technology has researched the concept of using a hybrid-propulsion system for a high-altitude long-endurance UAV [7]. These projects illustrate that various organizations are evaluating hybrid-electric propulsion systems for aerospace applications [8].

A conceptual design of a small UAV with a parallel hybrid-electric propulsion system, the application of a rule-based controller to the hybrid-electric system, and simulation results are provided. The proposed parallel hybrid-electric propulsion system takes advantage of the two types of propulsion (i.e., ICE and EM) while allowing some compromise (i.e., reduced payload mass). The two-point conceptual design includes an ICE sized for cruise speed and an EM and battery pack sized for endurance speed. A constrained optimization formulation is used to size the wing and the propulsion system components. The power required at the endurance speed is minimized to reduce the mass and volume of the battery pack. A rule-based controller for the hybrid-electric system incorporates ideal operating line (IOL) concepts developed by previous researchers [9–11]. A Simulink model was created to compare energy use results between the various configurations. A neural network controller that further improves on the rule-based controller is explained in other papers [12,13].

II. Hybrid-Electric Vehicle Configurations and Operating Strategies

The mechanical configuration of an HEV can be classified into two main categories: series and parallel (see Fig. 1) [1,14,15]. The ICE in a series configuration acts as an auxiliary power unit to drive a generator that provides power to the energy storage system or the EM. Only the EM is connected to the mechanical drive train. The ICE is not connected to the mechanical drive path which allows it to be operated in an optimum torque and speed range. However, large energy conversion losses exist between the mechanical and electrical systems diminishing the overall system efficiency [16]. Also, the EM has to be sized for the maximum power required [14]. The series configuration is useful for low-speed, high-torque applications such as buses and aircraft tow tractors. In a parallel configuration, each energy source or converter can provide propulsion energy because the ICE and EM are both mechanically connected to the drive train. The torque of the EM can supplement the torque of the ICE, or an additional ICE torque can operate the EM as a generator to recharge the battery pack. Because of the mechanical coupling, energy converters such as gas turbines with a relatively large turn-on/off time cannot be used in a parallel configuration [17]. The speed of the drive train is not always the optimum speed for the engine, but the energy conversion losses are minimized. The ICE and EM can be sized smaller than in a series configuration, and the EM is used as the generator so that a separate generator is not required. The parallel configuration is used in most FutureTruck [18–20] competition vehicles and in the Honda Insight and Civic. The parallel and series hybrid configurations are the traditional configurations, but others have been used such as the series-parallel configuration used in the Toyota Prius and the Nissan Tino [21]. The different configurations each have their advantages and disadvantages, and the configuration is dictated by the application and the type of energy source or converter.

An estimate was completed between a parallel and a series configuration for a small UAV [12]. The parallel configuration is lighter by ≈1.1 kg (≈2.5 lbs), or 8%, of the proposed UAV's gross weight of 13.6 kg (30 lbs). The extra weight for the series configuration is primarily due to the required generator and the larger EM. The series configuration and controller are mechanically and electronically simpler, but the disadvantages are the weight penalty and the larger energy conversion losses. Harmats also concluded that the parallel configuration was more effective than the series configuration for a hybrid-electric propulsion system (solar power/EM/ICE) for a UAV [7]. The parallel configuration contains a more complicated controller and clutch/gearing mechanism but weighs less and has less energy conversion losses which are significant considerations for the UAV design. During flight, the UAV with the parallel hybrid-electric propulsion system allows the vehicle to be propelled directly with the ICE, EM, or both. The parallel configuration is used for the hybrid-electric UAV due to the advantages of a parallel configuration for analogous applications, the weight savings, less energy conversion losses, and because of the parallel HEV experience at the University of California—Davis.

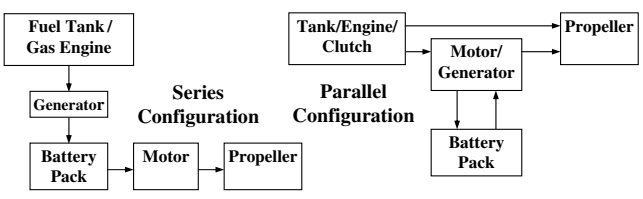

Fig. 1 Series and parallel hybrid-electric configurations.

In addition to the two primary HEV configurations, three overarching operating strategies are used for the energy management of an HEV: electric only, charge sustaining (CS), and charge depleting (CD) [22]. The electric-only strategy depends on the ICE turn-on speed, the size of the battery pack, and the amount of low-speed operation. The other two strategies are the hybrid approaches. The CS hybrid strategy often uses a "thermostat" approach with an attempt to maintain the battery state of charge (SOC) at a certain level. The thermostat method allows the vehicle to be similar to conventional vehicles where no off-board charging is required. In contrast to the CS strategy, the CD strategy allows the battery SOC to decrease maximizing the use of electricity from off-board charging.

The hybrid-electric UAV (HEUAV) uses a mix of the operating strategies depending on the mission and the intent of the operator. For electric-only operation (i.e., reduced signature), the HEUAV is flown at a relatively slow endurance speed. For hybrid-electric operation, a relatively large battery pack cannot be used due to weight limitations, and so a purely CD strategy cannot be used. A purely CS strategy will limit the time on station and the time for electric-only operation. Therefore, a combination of the charging strategies is used depending on the mission.

III. Conceptual Design of a Parallel Hybrid-Electric Propulsion System

Many HEVs are conversions from stock vehicles where the original power train is removed and the appropriate components for the hybrid-electric power train are installed. Although the design for the HEUAV could take the same approach by using a large scale model aircraft or a manufacturer's UAV, this section steps through a conceptual design process for sizing the wing and the propulsion system components. The background provides a fundamental understanding of the requirements and tradeoffs for the hybrid-electric propulsion system. Compromise in the design such as a reduced payload mass is necessary to allow for the larger mass of the hybrid-electric propulsion system. The information in this section was presented at the Unmanned Systems North America 2004 Symposium [23].

The conceptual design approach for aircraft is well described in Anderson, Raymer, Stinton, and Corke [24–27]. Key design variables such as wing lift coefficient, wing loading, power-to-weight ratio, and aspect ratio are optimized in the conceptual design process. The literature reveals that defense contractors and universities have devoted much effort to the subject of conceptual design [28].

Conceptual design is a multidisciplinary endeavor, but the focus here is the initial sizing of the wing and the hybrid-electric propulsion system components for a conventional high-wing UAV. The HEUAV sizing problem is a constrained optimization formulation. The MATLAB optimization routine uses a sequential quadratic programming method. A quasi-Newton updating method is used at each iteration, and the solution of a quadratic programming subproblem is then computed and used in a line search procedure.

The size of the wing and the propulsion system components for the HEUAV are determined using a flowchart (see Fig. 2). To begin, the

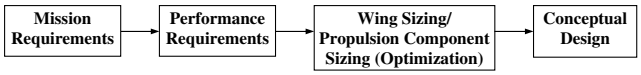

Fig. 2 Hybrid-electric propulsion system sizing flowchart.

primary mission requirements for the UAV are determined. Once the mission requirements are specified, performance parameters required to satisfy the mission are then established. The size of the wing and the propulsion system components are estimated based on the performance parameters. The conceptual design would undergo iterations before a detailed design is obtained.

A. ISR Mission Requirements

The small HEUAV is sized for a typical ISR mission. A typical flight profile would be to take off, climb to approximately 1500 m (≈5 kft) mean sea level (MSL), cruise for an hour to the location of interest, fly at endurance speed (i.e., electric-only operation) while on station for an hour conducting ISR, and then return to base and land. A descent and climb could also be added before and after the ISR segment to decrease the line-of-sight distance to the area of interest. The typical mission is used to illustrate the concepts, but the sizing process could be easily adapted to other missions.

B. HEUAV Performance Requirements

Performance requirements to satisfy the ISR mission are used to size the wing and the propulsion system components (see Table 1). The size of the hybrid-electric system components are based on the following regimes of operation [15,29]: 1) takeoff power provided by the ICE or the ICE and EM, 2) climbing power provided by the ICE or the ICE and EM, 3) maximum speed power provided by the ICE and EM, 4) cruise power provided by the ICE (a margin is needed to recharge the batteries during CS operation), 5) endurance power provided by the EM for electric-only operation, and 6) missed approaches and emergency power provided by the ICE and EM. The ICE is sized for the cruise speed and the EM is sized for the endurance speed. Please note that the cruise speed shown in Table 1 is greater than the theoretical cruise speed ($V_{\text{Cruise}} = 1.32 \cdot V_{\text{Endurance}}$) which increases the fuel consumption at the cruise speed. However, flying at a speed greater than the theoretical cruise speed minimizes the time required to reach the area of interest and the power required at the slower endurance speed [24]. The power requirements for different mission segments were analyzed in the typical ISR mission.

C. Wing and Propulsion System Component Sizing

The sizing of the wing and the propulsion system components are determined from the performance parameters. Because of the potentially large number of variables involved, several were chosen as the key parameters for the sizing process such as the wing loading, aspect ratio, maximum lift coefficient, stall speed, and endurance speed. For the constrained optimization formulation, the objective function to be minimized is the power required at the endurance speed. By minimizing the power required at the endurance speed, the battery pack mass is minimized permitting a feasible payload mass.

Since the emphasis of the mission is on the ISR segment, the EM size and battery mass are first determined to satisfy the one hour of endurance while on station using electric-only propulsion power. The power required to fly at the endurance speed is given by [24]

$$J = \text{PR} = \eta_{\text{Prop}} \cdot P_{\text{EM}} = \sqrt{\frac{2 \cdot W^3 \cdot C_D^2}{\rho \cdot S \cdot C_L^3}} = W \cdot \sqrt{\frac{2 \cdot W \cdot C_D^2}{\rho \cdot S \cdot C_L^3}}$$

$$= W \cdot \sqrt{\frac{2}{\rho} \cdot \left(\frac{W}{S}\right)} \cdot \frac{4 \cdot C_{D,0}}{(3 \cdot C_{D,0} \cdot \pi \cdot e \cdot \text{AR})^{0.75}} \tag{1}$$

The power required at the endurance speed is minimized with a small wing loading, W/S, and a large aspect ratio if initial estimates for W, $C_{D,0}$, and e are available. To minimize the power, the result is an aircraft that has a large wing area and aspect ratio such as a glider. This type of aircraft would be the most beneficial for sizing the electric system but limits other performance parameters such as the maximum speed. A compromise must be made between this geometry and a smaller wing and aspect ratio. To determine the power required from the batteries, it is noted that the power PR given by Eq. (1) does not include the propeller efficiency, motor efficiency, and the power required for the payload, avionics, and flight control system.

The parameter $C_L^{3/2}/C_D$ in Eq. (1) is referred to as the endurance parameter and is found in the literature as the key parameter for solar aircraft or any aircraft with a mission requiring it to fly at or near the endurance speed [30]. Since the ISR mission requires the HEUAV to fly near the endurance speed, the endurance parameter is critical.

Three constraints are required to complete the constrained optimization formulation. The aspect ratio expressed in terms of the wing loading and the endurance speed gives the first constraint [24]:

$$\sqrt{\text{AR}} = \left[\frac{2}{\rho} \cdot \left(\frac{W}{S}\right) \cdot \sqrt{\frac{1}{3 \cdot C_{D,0} \cdot \pi \cdot e}}\right] \cdot \frac{1}{V_{\text{Endurance}}^2} \tag{2}$$

The second constraint involves the wing loading, stall speed, and the maximum lift coefficient [24]:

$$\frac{W}{S} = \frac{\rho \cdot V_{\text{Stall}}^2 \cdot C_{L,\max}}{2} \tag{3}$$

The stall speed, for this application and other low-speed aircraft, determines the desired wing loading [24]. The landing distance, considered not to be critical for this application, can also determine the wing loading. A safety speed margin of several knots is desired between the stall and endurance speeds to account for wind turbulence and other disturbances.

The third constraint determines the size of the gasoline ICE. A margin of ≈125% provides additional power from the ICE to operate the EM as a generator to recharge the batteries during CS operation and to provide power for the payload, avionics, and flight control system. The expression for the cruise power required can be expressed as

$$\text{PR} = P_{\text{ICE}} \cdot \eta_{\text{Prop}} \cdot 0.8 = V_{\text{Cruise}} \cdot \left[0.5 \cdot \rho \cdot V_{\text{Cruise}}^2 \cdot S \cdot C_{D,0} + \frac{S}{0.5 \cdot \rho \cdot V_{\text{Cruise}}^2 \cdot \pi \cdot e \cdot \text{AR}} \cdot \left(\frac{W}{S}\right)^2\right] \tag{4}$$

where $\text{PR} = V_{\text{Cruise}} \cdot \text{TR}$ at cruise speed. For this application, the cruise speed is not necessarily the theoretical cruise speed but is a desired cruise speed to minimize the time required to approach the area of interest or a speed that corresponds to the intended mission. Using $S = S \cdot W/W$, Eq. (4) becomes

$$\text{PR} = P_{\text{ICE}} \cdot \eta_{\text{Prop}} \cdot 0.8 = 0.5 \cdot \rho \cdot V_{\text{Cruise}}^3 \cdot W \cdot C_{D,0} \cdot \frac{S}{W} + \frac{W}{0.5 \cdot \rho \cdot V_{\text{Cruise}} \cdot \pi \cdot e \cdot \text{AR}} \cdot \left(\frac{W}{S}\right) \tag{5}$$

For the maximum speed, the EM and ICE are both used to provide propulsion power. The EM can tolerate an overtorque for short durations and so the expression for the maximum speed is the same as

Table 1 Performance requirements

Parameter	Value
Cruise speed, m/s	23–28 (45–55 kn)
Endurance speed, m/s	10–13 (20–25 kn)
Maximum speed, m/s	31–33 (60–65 kn)
Rate-of-climb, m/s	2.0 (400 ft/ min)
Time for cruise (range), hr	1.0
Time at endurance speed, hr	1.0
Takeoff distance, m	<30 (100 ft)
Avionics and payload power, W	75
Payload mass, kg	1.5–3.0 (3.3–6.6 lbs)

Eq. (5) except PR $= P_{\text{ICE}} \cdot \eta_{\text{Prop}} +$ overtorque $\cdot \eta_{\text{Prop}} \cdot P_{\text{EM}}$. Typical values for the overtorque factor are 1.5–2.0.

The objective function and the third constraint form the foundation for a two-point conceptual design for the HEUAV. The optimization routine determines the optimum design between the two design points.

D. Conceptual Design Results

The conceptual design results based on the constrained optimization formulation led to the results shown in Table 2 for an altitude of 1525 m (5 kft) MSL. Limits were placed on the optimized variables and the results show that the optimization routine used the lowest wing loading available. The size of the wing is directly related to the wing loading. A large wing is desired, but other performance parameters must be considered along with the structural, weight, and low-observable requirements. Limits were placed on the maximum lift coefficient to obtain results that would permit a standard NACA, Eppler, or Selig airfoil to be used [31,32]. Other high lift wings could be used such as NASA's low Reynolds number LRN-1-1010 airfoil that was utilized in the Navy's low altitude unmanned research aircraft (LAURA) project [33]. The optimization results either meet or exceed the performance requirements listed in Table 1. The power requirements for each mission phase are shown and are used to size the different components. A smaller ICE and less fuel can be used for the HEUAV as compared to the original (ICE-only) configuration. The HEUAV requires 25% less fuel than the original configuration for the same mission but with a reduced payload (1.9 vs 3.0 kg).

The hybrid-electric propulsion system is a two-point design with the electric system sized for endurance speed and the ICE sized for a desired cruise speed. The two design points are shown in Fig. 3. The endurance speed from the optimization routine is less than the stall speed which would prevent the HEUAV from flying precisely at the theoretical endurance speed but was permitted to minimize the required endurance power. The power required to fly several knots above the stall speed instead of precisely at the endurance speed is minimal. The EM and battery pack are sized for the endurance speed with additional power for the avionics, payload, and flight control system. The desired cruise speed is greater than the theoretical cruise speed. More fuel is consumed while flying at a higher cruise speed, but the time required to reach the area of interest is minimized. If the time to fly to the area of interest is not critical, then the UAV may be flown at the theoretical cruise speed to further increase the range. The gasoline ICE is sized for a desired cruise speed of 25.7 m/s (50 kn) which requires ≈500 W not including the inefficiencies of the propulsion system and the margin required for the CS operation.

Table 2 HEUAV optimization and conceptual design results

Parameter	Value
Optimization routine results	
Aspect ratio	14.6
Wing loading, N/m^2	90 (30 oz/ft^2)
Maximum lift coefficient, $C_{L,\max}$ (finite wing)	1.25
Oswald efficiency factor	0.85
Zero-lift drag coefficient	0.036
Stall speed, m/s	11.6 (22.7 kn)
Endurance speed, m/s	9.1 (17.7 kn)
EM power at endurance speed, W	114
ICE power estimate at cruise speed, W	837 (1.1 hp)
Conceptual design results	
Design altitude, m MSL	1525 (5 kft)
HEUAV mass, kg	13.6 (30 lbs)
Wing area, m^2	1.48 (1.59 ft^2)
Wing span, m	4.65 (15.3 ft)
Wing chord, m	0.32 (12.5 in)
Endurance parameter	20.4
Max L/D ratio	16.4
PR for takeoff, W[a]	503
PR for climb, W[a]	356
PR for cruise, W[a]	502
PR for endurance, W[a]	85
PR for max speed, W[a]	852
Nominal propeller efficiency, %	75
Original fuel mass, kg	2.0 (71 oz)
HEUAV fuel mass, kg	1.5 (53 oz)
Original payload mass, kg	3.0 (6.6 lbs)
HEUAV payload mass, kg	1.9 (4.2 lbs)
Original ICE power required, W	1230 (1.7 hp)
HEUAV battery mass, kg[b]	2.2 (4.9 lbs)
HEUAV battery storage, Wh[b]	220

[a]The PR does not include propulsion system inefficiencies or the PR for the avionics, flight control system, and payload.
[b]The battery storage requirement includes the power needed for the avionics and payload.

The conceptual design results can be further viewed using weight fractions. The weight of the UAV can be expressed using weight fractions as [25]

$$W_0 = \frac{W_{\text{Payload}}}{1 - \frac{W_{\text{Fuel}}}{W_0} - \frac{W_{\text{Empty}}}{W_0}} \tag{6}$$

Since the empty weight includes the propulsion system, Eq. (6) can be modified to separate the propulsion system weight:

$$W_0 = \frac{W_{\text{Payload}}}{1 - \frac{W_{\text{Fuel}}}{W_0} - \left(\frac{W_{\text{Empty}} - W_{\text{Propulsion}}}{W_0}\right) - \frac{W_{\text{Propulsion}}}{W_0}} \tag{7}$$

The term, $(W_{\text{Empty}} - W_{\text{Propulsion}})/W_0$, is the glider weight fraction. Equation (7) is used to compare the weight fractions of the original configuration to the hybrid-electric configuration. The propulsion system weight fraction for the original configuration includes a larger ICE, generator, and the propeller. For the parallel hybrid-electric configuration, the propulsion system weight fraction includes the downsized ICE, clutch, batteries, EM, and the propeller. The fuel weight fraction, W_{Fuel}/W_0, is determined by computing the amount of fuel needed for each mission segment using estimates and the well-known Breguet equation [24]. For the HEUAV, no fuel is used during the endurance mission segment because only electric power is required. The amount of fuel required for the mission is used to size the fuel tank for the original and the HEUAV configurations.

The weight fractions required for the original and HEUAV configurations are shown in Fig. 4. The glider weight fraction is statistically estimated from several UAVs in the same weight class with an empty weight of 0.63. The propulsion weight fraction for the original configuration is less than the HEUAV configuration, and the payload weight fraction is reduced for the HEUAV configuration. The fuel weight fraction is 0.11 for the HEUAV and 0.15 for the original configuration. The advantages of the HEUAV configuration (i.e., reduced signature and less fuel) must be weighed against the loss in payload mass for a particular mission. The weight fractions for

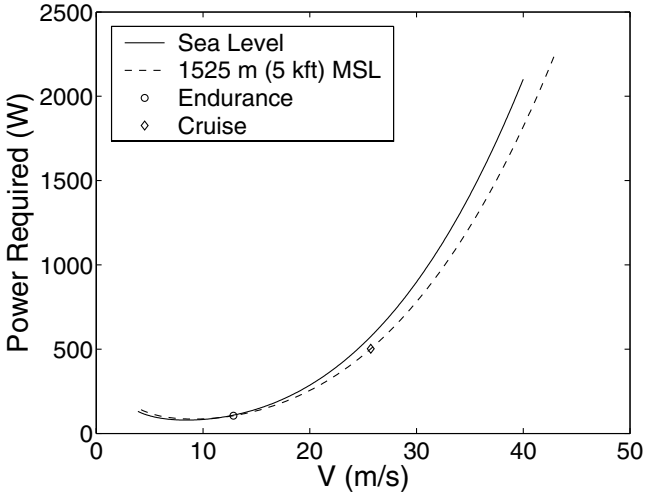

Fig. 3 Power required for the HEUAV at sea level and 1525 m (5 kft) MSL.

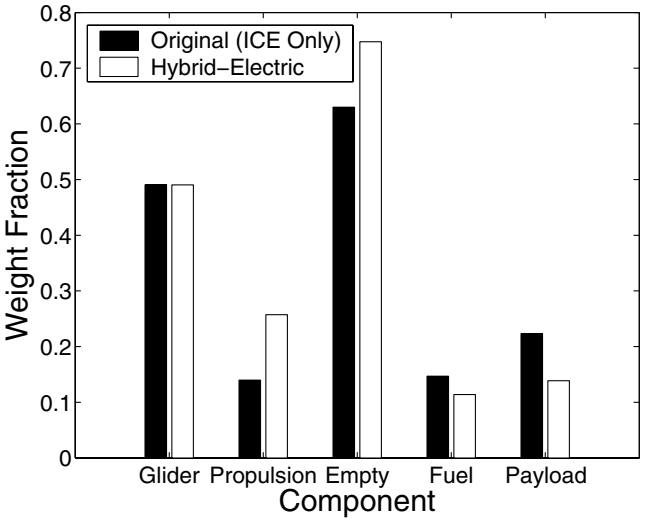

Fig. 4 Weight fraction comparison between configurations, $W_0 = 133$ N (30 lbs).

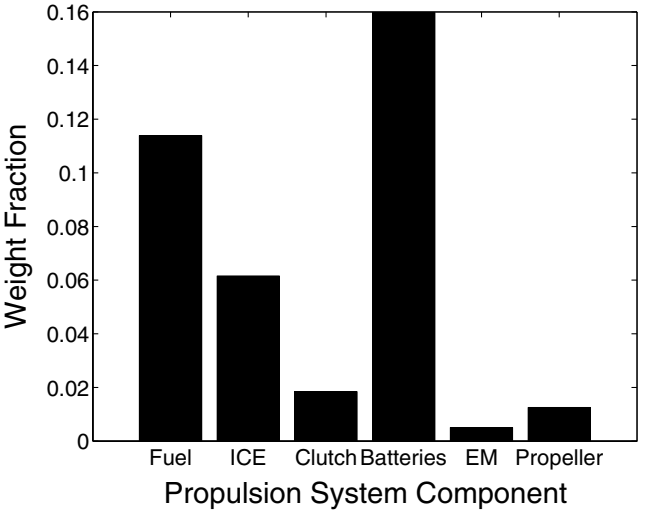

Fig. 5 HEUAV propulsion system weight fractions, $W_0 = 133$ N (30 lbs).

the HEUAV propulsion system components are shown in Fig. 5. Less fuel is required for the HEUAV, but the battery weight is significant with a weight fraction of 0.16.

Commercial off-the-shelf components are matched to the optimization simulation results (see Table 3). Nominal design values based on the results from the optimization routine and the components in Table 3 are used for the HEUAV propulsion system simulations. The ICE, EM, and battery pack are slightly larger than required but will ensure the power requirements are met for the intended missions.

A two-stroke gasoline engine was matched to the optimization results because the fuel is available at military installations and because the engines are readily available. Two-stroke engine simulations are presented in another paper [13]. A four-stroke gasoline engine is used in subsequent simulations in this paper, but the more efficient engine is heavier and the payload capacity is decreased. Attempts are being made to design small heavy fuel engines for UAVs so that they use similar fuels as other military vehicles instead of gasoline. D-Star Engineering has designed a 0.07 kW and a larger 1 kW diesel engine intended for UAVs [34]. For the purposes of the conceptual design, typical performance of a two-stroke gasoline engine was used, but the conceptual design approach could be easily adapted to other types of engines.

IV. Control Algorithms for Hybrid-Electric Propulsion Systems

The hybrid-electric vehicle operating strategies (i.e., electric only, CS, and CD) are overarching approaches. For each operating strategy, control algorithms are used to optimize the energy or power use of the propulsion system. In addition to rule-based strategies, several advanced control approaches have been reported in the literature for the control of HEV power trains in automotive applications: 1) optimal control, 2) fuzzy logic, 3) adaptive control, 4) nonlinear control, and 5) genetic algorithms. The advanced control algorithms are not a replacement for the rule-based algorithms but are a supplement to the experience of the designer or researcher. A brief overview of rule-based and advanced algorithms and their application to the control of HEV power trains are given in [12]. The goal of an advanced control system is to use a minimal amount of energy by finding the best combination of motor torque and engine torque as a function of rotational speed, battery SOC, torque demand,

Table 3 HEUAV commercial off-the-shelf components

Parameter	Value	Parameter	Value
Airframe	Conventional high-wing aircraft	Battery pack	Ultralife UBI-2590 (2 in parallel)
Mass, kg	13.6 (30 lbs)	Type	Li-ion, rechargeable
Oswald efficiency factor	0.85	Mass, kg	$2 \times 1.44 = 2.88$ (6.3 lbs)
Zero-lift drag coefficient	0.036	Voltage, nominal, V	14.4
Wing/airfoil	NACA 23012, E214, S2091, or SD7032	Voltage Range, V	12.0–16.4
$C_{L,\max}$	1.25 (3-D, $Re = 150$ k)	Capacity, C/2.5, Ah	$2 \times 10 = 20$
Aspect ratio	14.6	Energy density, Wh/kg	100
Wing area, m^2	1.48 (15.9 ft^2)	Recommended discharge current, A	$2 \times 8 = 16$
Wing span, m	4.65 (15.3 ft)	Electric motor (3.7:1 gearbox)	Aveox 2739/3Y brushless DC
Wing chord, m	0.32 (1.25 in.)	Mass, kg	0.16 (5.6 oz)
Payload		Max peak current, A	30
Original payload mass, kg	2.9 (6.4 lbs)	Max continuous current, A	22
HEUAV payload mass, kg	1.7 (3.7 lbs)	Winding resistance, Ω	0.0817
Original generator/battery mass, kg	0.5	No load current, A	0.90
Avionics and payload power, W	75	Speed constant, rpm/V	1134
Engine (two-stroke, gasoline)	First place engines	Torque constant, N · m/A	0.0085
Displacement, cm^3	21 (1.3 in^3 (Original-35)	Motor constant, N · m/sqrt (W)	0.031
Mass, kg	1.13 (2.5 lb)	Maximum speed, rpm	50,000
Fuel tank mass, kg	1.53 (54 oz) (Original-2.10)	Propeller diameter, m (Maple)	0.46 (18 in)
Clutch (electromagnetic)	R. M. Hoffman Co.	Mass, kg	0.17 (6 oz)
Mass, kg	0.25 (0.55 lbs)	Horizontal and vertical stabilizer/airfoil	NACA 0009

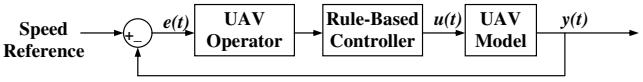

Fig. 6 Hybrid-electric propulsion system controller block diagram.

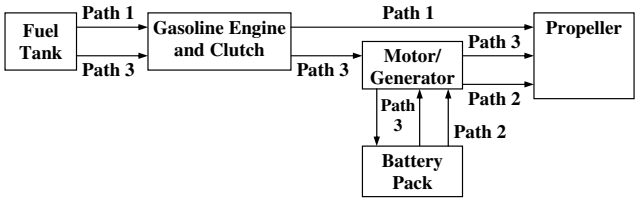

Fig. 7 Energy paths available in the parallel hybrid-electric propulsion system.

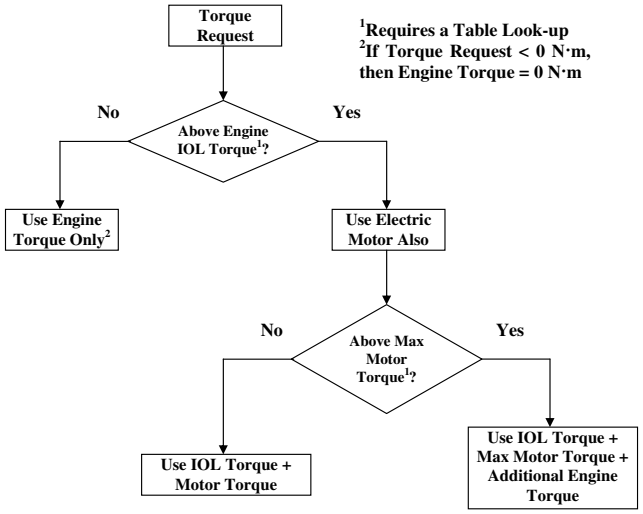

Fig. 8 Rule-based controller algorithm.

or other parameters. Of the hybrid-electric power train advanced control schemes appearing in the current literature, those based on artificial neural networks or fuzzy logic appear to be the most promising due to the relatively low computational resources needed and because an accurate power train propulsion model is not required (an accurate model is required for simulations). For a description of a neural network controller for the HEUAV, please refer to [13]. In this paper, a rule-based controller is used to control the HEUAV's propulsion system.

The rule-based strategies based on empirical data and experience have resulted in successful, reliable, and efficient HEV power trains. For the rule-based implementations, an attempt is made to operate the ICE and the EM in their most efficient regions. The ICE is operated on or near a line of maximum efficiency, the IOL, for the best efficiency during hybrid-electric operation [9,10]. Since operating one energy converter in its most efficient region usually does not permit the other one to operate in its most efficient region, tradeoffs must be made. The efficiency maps of the engine and electric motor, along with the expected energy conversion losses in the batteries and other components, are used by the control algorithms to minimize the energy use of the power train or propulsion system.

A block diagram of the HEUAV operator, controller, and model is shown in Fig. 6. For the HEUAV model, the speed is assumed to be the true velocity. Only the speed is used as a feedback variable because an increase in altitude with no throttle adjustments will result in a decrease in speed. It is assumed that a longitudinal control system maintains the UAV at the correct altitude.

The energy available in the small HEUAV is either from the gasoline or the electrical energy stored in the battery pack (see Fig. 7). To provide power to the propeller, the energy can take one of three paths. For path 1, energy stored within the gasoline is used by the ICE to deliver power directly to the propeller. Electrical energy can be delivered directly to the propeller via path 2. Path 3 uses the ICE and EM to recharge the battery pack. The stored electrical energy is delivered to the propeller at a later time and for the HEUAV, the electrical energy is assumed to be delivered to the propeller at endurance speed (electric-only operation).

The nonlinear efficiency maps for the ICE and EM are used by the rule-based controller. The maps are stored in tables, and interpolation is used to calculate the efficiency at specific points in the input space (i.e., demanded torque, rotational speed, etc.). The ICE efficiency maps are derived from estimates and engine manufacturer dynamometer tests. Four-stroke ICE efficiency maps are used in the simulations. The efficiency map for the four-stroke engine was derived from literature for the Honda GX31, 31 cm^3 (1.9 $in.^3$), engine. The best fuel consumption is $\approx$350 g/kWh or a maximum efficiency of $\approx$24%. The EM (Aveox 2739/3Y) efficiency map is derived from manufacturer data and has a maximum efficiency of $\approx$90%. The battery pack used in the simulations consists of two lithium-ion batteries (Ultralife UBI-2590) in parallel.

The flowchart for the rule-based controller is shown in Fig. 8. The simple rule-based controller has two inputs: demanded torque and rotational speed. The engine is operated on the IOL unless the demanded torque is less than the IOL torque or if the demanded torque is greater than the combined IOL torque and maximum motor torque [10,11]. Only the ICE generates torque if the demanded torque is less than the IOL torque. If the demanded torque is greater than the combined IOL torque and the maximum motor torque, then additional torque from the ICE is provided. The rule-based controller logic does not include any recharging so it is considered a CD strategy. If the mission requirements cannot be met with CD only, then a CS algorithm is used. The CS algorithm is based on the expected length of the mission and the battery SOC. A proportional-derivative (PD) controller, with the SOC as the input, is used to determine the amount of recharging required.

V. Flight Profiles and Simulation Results

A. Simulink Model and Flight Profiles

A Simulink model was developed to simulate the hybrid-electric UAV. The model (see Fig. 9) includes blocks for the flight profile, pilot/operator, propulsion system, and the UAV. The propulsion system block includes an option for the ICE-only configuration. The model also includes a standard atmosphere model to account for changes in temperature and density with altitude.

Two ISR missions are used to demonstrate the capabilities of the HEAUV and to compare the results between the hybrid-electric and original configurations. To show initial results for the various mission segments of a flight profile, a short one-hour ISR mission was generated (see Fig. 10). The flight profile consists of a takeoff, climb, cruise, endurance speed, high speed dash, descent, and landing. The cruise speed is 25.7 m/s (50 kn), and the endurance speed is 12.9 m/s (25 kn). At endurance speed, the hybrid-electric UAV operates in electric-only mode. The design altitude is 1525 m (5 kft) MSL and for this flight profile, the UAV takes off from 1219 m (4 kft) MSL. A climb and descent before the endurance mission segment simulate the flight over an obstacle.

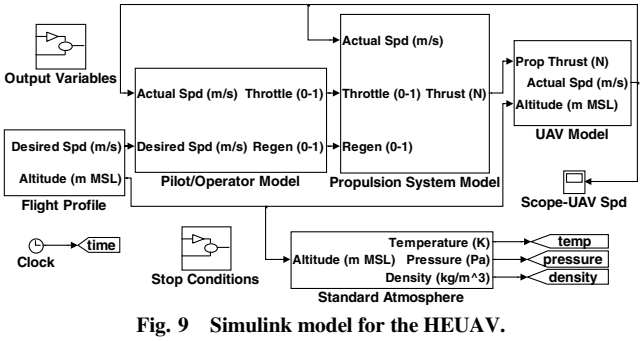

Fig. 9 Simulink model for the HEUAV.

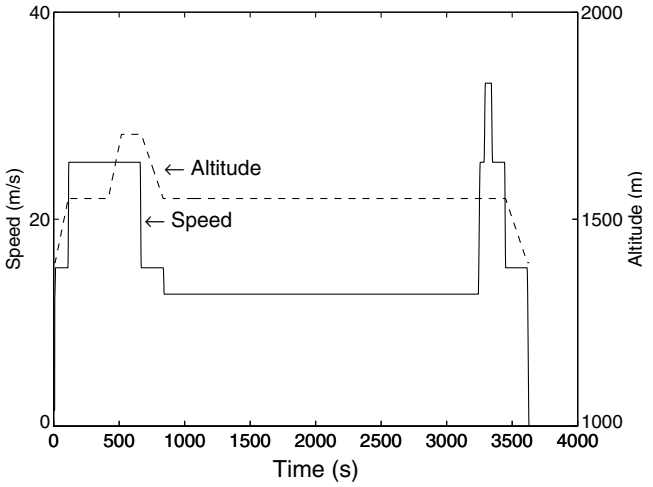

Fig. 10 One-hour flight profile.

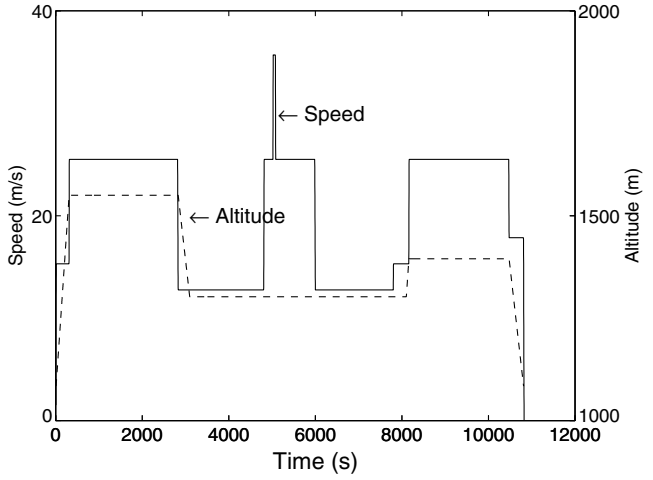

Fig. 11 Three-hour flight profile.

A three-hour ISR mission was also created (see Fig. 11) and includes a takeoff, climb, cruise, endurance speed, high speed dash, descent, and landing. The ISR segment is split into two different segments to simulate the observation of two different ground locations. The design altitude is 1525 m (5 kft) MSL and for this flight profile, the UAV takes off from 1067 m (3.5 kft) MSL.

B. Simulation Results for the One-Hour ISR Mission

The hybrid-electric propulsion system controller uses a CD strategy for the one-hour ISR mission. The rule-based strategy does not use any CS logic for this mission. The engine operating points for the hybrid-electric UAV are shown in Fig. 12 on an engine efficiency map (i.e., efficiency contours plotted vs torque and speed). The engine is operated near or on the IOL ($\approx$1.3 N $\cdot$ m) during the mission. A summary of the energy use for the one-hour ISR mission is listed in Table 4. Since the flight profile allows the HEUAV to take advantage of the CD logic, the HEUAV with the rule-based controller uses 54% less energy than the ICE-only configuration. The large decrease in energy use is due to the CD logic because the energy stored in the gasoline is not used to maintain the battery SOC.

C. Simulation Results for the Three-Hour ISR Mission

The rule-based controller uses CS throughout the three-hour mission to provide sufficient electrical energy during the two half-hour ISR mission segments. The amount of CS is dependent on the battery SOC because a PD controller is used to control the amount of extra torque the engine produces for recharging. Because of the PD

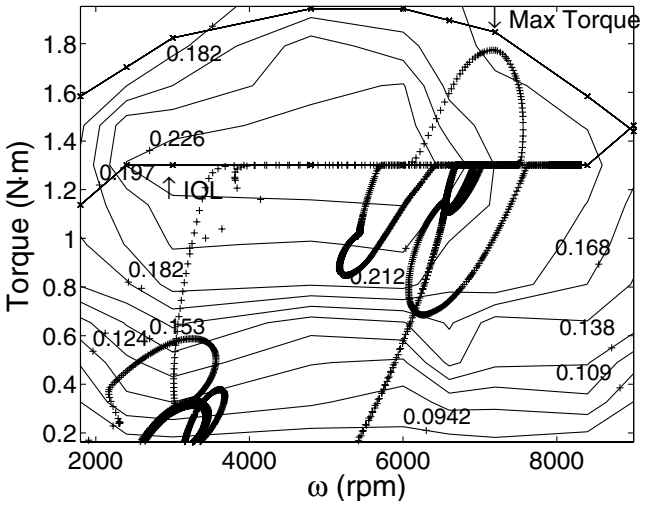

Fig. 12 Engine operating points, one-hour ISR mission, four-stroke engine, hybrid-electric configuration.

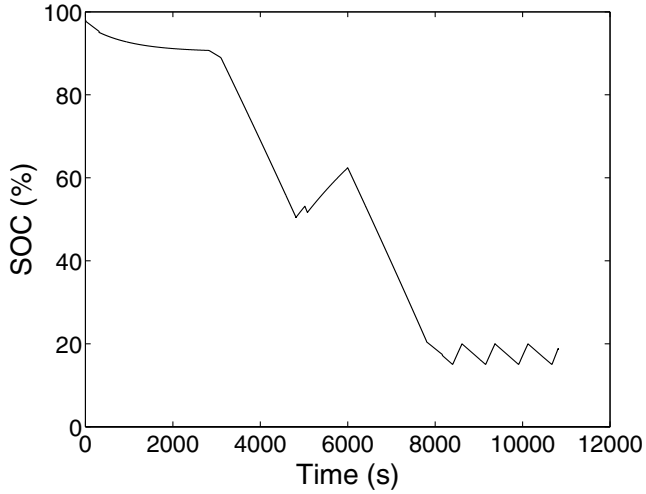

Fig. 13 Battery SOC, three-hour ISR mission, four-stroke engine, hybrid-electric configuration.

Table 4 Energy use summary for a one-hour mission, four-stroke engine

Energy type	Engine only	Hybrid electric
Fuel, g	192.3	70.4
Fuel, kWh	2.29	0.844
Electricity, kWh	N/A	0.202
Total, kWh	2.29	1.05

controller, the rate of charging increases as the SOC decreases. The logic keeps the SOC above 15% (see Fig. 13). The rule-based controller manages the storage of electrical energy sufficiently for the hybrid-electric system.

The engine operating points for the hybrid-electric UAV are shown in Fig. 14 on an engine efficiency map. The engine is operated near or on the IOL ($\approx$1.3 N $\cdot$ m) for specific segments of the mission. However, due to the CS operation, the engine torque is increased above the IOL during several mission segments to provide extra torque to operate the EM as a generator.

The energy use for the three-hour ISR mission using the different configurations is shown in Table 5. The energy use for the HEUAV using the rule-based controller is 22% less than the original configuration. Since CS is required for this mission, the energy savings is less than for the shorter one-hour mission.

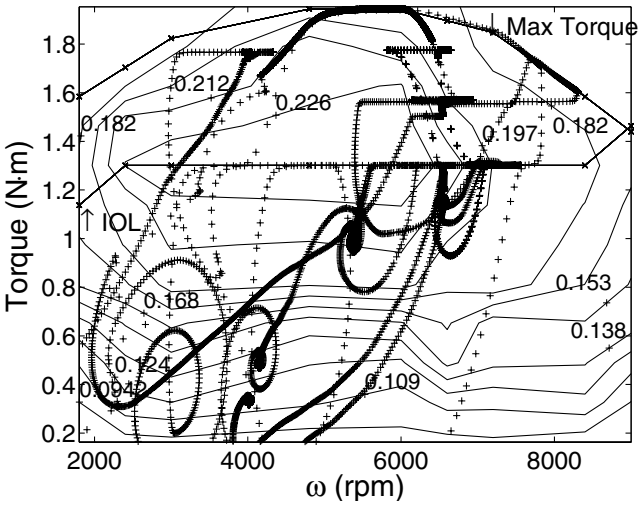

Fig. 14 Engine operating points, three-hour ISR mission, four-stroke engine, hybrid-electric configuration.

Table 5 Energy use summary for a three-hour ISR mission, four-stroke engine

Energy type	Engine only	Hybrid electric
Fuel, g	779.3	582.1
Fuel, kWh	9.27	6.98
Electricity, kWh	N/A	0.240
Total, kWh	9.27	7.22

VI. Conclusions and Future Work

A conceptual design of a small UAV with a parallel hybrid-electric propulsion system, the application of a rule-based controller to the hybrid-electric system, and simulation results were provided. The hybrid-electric UAV would be useful for military, homeland security, or disaster-monitoring missions involving ISR. The two-point conceptual design includes an internal combustion engine sized for cruise speed and an electric motor and lithium-ion battery pack sized for endurance speed. The hybrid-electric propulsion system uses less energy than the original configuration due to the available energy in the battery pack. The hybrid-electric UAV also has a reduced thermal and acoustic signature than a purely gasoline-powered UAV. The advantages of the hybrid-electric UAV for a specific mission must be weighed against the loss in payload mass due to the heavier propulsion system.

Future work related to this research includes dynamometer testing to evaluate advanced UAV propulsion systems, variable-pitch propeller testing, and intelligent controller design. As UAVs are used for more applications, computerized dynamometer test stands will be needed to test more fuel efficient propulsion systems. A fixed-pitch propeller was used in the hybrid-electric UAV model, but it operates at its peak efficiency over a short range of advance ratio. For the hybrid-electric UAV, the advance ratio was similar at cruise and endurance speed. However, at other speeds that may be required for various missions, the propeller may not operate near its maximum efficiency. A variable-pitch propeller permits a high efficiency over a wider range of advance ratio. The desired pitch could be an output from the hybrid-electric propulsion system controller. The rule-based controller provided efficient use of the energy available onboard the UAV. However, intelligent control algorithms such as neural networks and fuzzy logic could further minimize the energy use of the hybrid-electric UAV.

Acknowledgments

This research was supported by Integrative Graduate Education and Research Traineeship (IGERT) funding from the National Science Foundation (NSF). Technical support was provided by engineers from UAV propulsion system component manufacturers including Ultralife Batteries, Aveox, and First Place Engines.

References

[1] Chan, C. C., and Chau, K. T., *Modern Electric Vehicle Technology*, Oxford Univ. Press, Oxford, England, U.K., 2001.

[2] Aldridge, E. C., and Stenbit, J. P., "Unmanned Aerial Vehicles Roadmap: 2002–2027," Office of the Secretary of Defense, Dec. 2002.

[3] Perazzola, C., "Tomorrow's Ground Power Today," *Proceedings of the SAE TOPTEC Conference*, Society of Automotive Engineers, Warrendale, PA, June 2002.

[4] Wilson, S. B., "Micro Air Vehicle Project," *Proceedings of the DARPATech Symposium*, Anaheim, CA, 2002.

[5] Norris, G., "Hydrogen Power Offers Leap Forward for UAVs," Flight International, Sept. 2003, p. 33.

[6] Bennett, E., "NASA's Helios Prototype-Soaring to a New Record," *SAMPE Journal*, Vol. 38, No. 3, 2002, pp. 41–47.

[7] Harmats, M., and Weihs, D., "Hybrid-Propulsion High-Altitude Long-Endurance Remotely Piloted Vehicle," *Journal of Aircraft*, Vol. 36, No. 2, 1999, pp. 321–331.

[8] Wilson, J. R., "UAVs: A Worldwide Roundup," *Aerospace America*, Vol. 41, June 2003, pp. 30–35.

[9] Francisco, A. B., M.S. Thesis, "Implementation of an Ideal Operating Line Control Strategy for Hybrid Electric Vehicles," Dept. of Mechanical and Aeronautical Engineering, University of California—Davis, Davis, CA, 2002.

[10] Frank, A. A., "Control Method and Apparatus for Internal Combustion Engine Electric Hybrid Vehicles," United States Patent and Trademark Office Patent Database, Patent No. 6,054,844, The Regents of the University of California, 2000.

[11] Frank, A. A., "Charge Depletion Control Method and Apparatus for Hybrid Powered Vehicles," United States Patent and Trademark Office Patent Database, Patent No. 5,842,534, The Regents of the University of California, 1998.

[12] Harmon, F. G., Ph.D. Dissertation, "Neural Network Control of a Parallel Hybrid-Electric Propulsion System for a Small Unmanned Aerial Vehicle," Dept. of Mechanical and Aeronautical Engineering, University of California—Davis, Davis, CA, 2005.

[13] Harmon, F. G., Frank, A. A., and Joshi, S. S., "The Control of a Parallel Hybrid-Electric Propulsion System for a Small Unmanned Aerial Vehicle Using a CMAC Neural Network," *Neural Networks*, Vol. 18, 2005, pp. 772–780.

[14] Husain, I., *Electric and Hybrid Vehicles Design Fundamentals*, CRC Press, Boca Raton, FL, 2003.

[15] Burke, A. F., "Hybrid/Electric Vehicle Design Options and Evaluations," SAE Paper SP-915, 1992, pp. 53–77.

[16] Kim, C., NamGoong, E., Lee, S., Kim, T., and Kim, H., "Fuel Economy Optimization for Parallel Hybrid Vehicles with CVT," SAE Paper 1999-01-1148, 1999.

[17] Johnston, B., McGoldrick, T., Funston, D., Kwan, H., Alexander, M., Alioto, F., Culaud, N., Lang, O., Mergen, H. A., Carlson, R., Frank, A., and Burke, A., "The Continued Design and Development of the University of California—Davis FutureCar," SAE Paper 980487, 1998.

[18] Kleback, B., Inman, S., and Noss, R., "Design and Development of the 2002 Penn State University Parallel Hybrid Electric Explorer, the Wattmuncher," SAE Paper 2003-01-1258, 2003.

[19] Meyr, N., Carde, C., Nitta, C., Garas, D., Garrard, T., Parks, J., Vaughn, C., Bangar, C., Francisco, A., Duvall, M., and Frank, A., "Design and Development of the 2002 UC Davis FutureTruck," SAE Paper 2003-01-1263, 2003.

[20] Bond, C., Boyle, K., Freeman, N., Orr, D., Brewin, D., Christenson, R., Cannon, M., and Checkel, D., "Design and Development of the 2003 University of Alberta Hybrid Electric Vehicle," SAE Paper 2003-01-1268, 2003.

[21] Matsuo, I., Nakazawa, S., Maeda, H., and Inada, E., "Development of a High-Performance Hybrid Propulsion System Incorporating a CVT," SAE Paper 2000-01-0992, 2000, pp. 1–9.

[22] Schurhoff, R. W., M.S. Thesis, "The Development and Evaluation of an Optimal Powertrain Control Strategy for a Hybrid Electric Vehicle," Dept. of Mechanical and Aeronautical Engineering, University of California—Davis, Davis, CA, 2002.

[23] Harmon, F. G., Frank, A. A., and Chattot, J. J., "Parallel Hybrid-Electric Propulsion System for an Unmanned Aerial Vehicle," *Proceedings of the AUVSI's Unmanned Systems North America Symposium*, AUVSI, Arlington, VA, 2004.

[24] Anderson, J. D., *Aircraft Performance and Design*, McGraw–Hill, Boston, MA, 1999.

[25] Raymer, D. P., *Aircraft Design: A Conceptual Approach*, AIAA, Washington, D.C., 1992.
[26] Stinton, D., *The Design of the Airplane*, 2nd ed., AIAA, Reston, VA, 2001.
[27] Corke, T. C., *Design of Aircraft*, Prentice–Hall, Upper Saddle River, NJ, 2003.
[28] Raymer, D. P., *Aircraft Design: A Conceptual Approach*, AIAA, Reston, VA, 1999.
[29] Ehsani, M., Rahman, K. M., and Toliyat, H. A., "Propulsion System Design of Electric and Hybrid Vehicles," *IEEE Transactions on Industrial Electronics*, Vol. 44, No. 1, 1997, pp. 19–27.
[30] Youngblood, J. W., and Talay, T. A., "Solar-Powered Airplane Design for Long-Endurance, High-Altitude Flight," *Proceedings of the AIAA 2nd International Very Large Vehicles Conference*, AIAA, New York, 1982.
[31] Selig, M. S., Donovan, J. F., and Fraser, D. B., *Airfoils at Low Speeds*, H. A. Stokely, Virginia Beach, VA, 1989.
[32] Eppler, R., *Airfoil Design and Data*, Springer–Verlag, Berlin, 1990.
[33] Siddiqi, S., Evangelista, R., and Kwa, T. S., "The Design of a Low Reynolds Number RPV," *Low Reynolds Number Aerodynamics*, Springer–Verlag, Berlin, 1989.
[34] Dev, S. P., "JP-8/Battery Hybrid Propulsion and Power for Small UAVs and UGVs," *Proceedings of the AUVSI's 30th Annual Unmanned Systems Symposium and Exhibition*, AUVSI, Arlington, VA, 2003.